Available online at www.sciencedirect.com
SCIENCE DIRECT®
Journal of the European Ceramic Society 25 (2005) 1647–1655
www.elsevier.com/locate/jeurceramsoc

Correlation of microstructures with electrical performance of Ag-based metal electrode–PZT electroceramic interfaces

L.J. Ecclestone, I.M. Reaney, W.E. Lee*

Department of Engineering Materials, University of Sheffield, Sheffield S1 3JD, UK

Received 11 February 2004; received in revised form 24 May 2004; accepted 31 May 2004
Available online 13 August 2004

Abstract

The microstructures of 8 model Ag-based electrode pastes, fired on to PZT using commercial firing schedules, have been examined using SEM with EDS, and the electrical performance of these systems investigated. The effects of three different bonding additives (Bi_2O_3, CuO, and a lead boro-aluminosilicate glass frit) were investigated both individually and together. The additives were found to be vital for good bonding. In unfritted systems eutectic reactions between the additives, the electrode Ag, and the PZT dominated the microstructural evolution, the loss of Pb from the ceramic being of particular importance. In fritted pastes the glass frit dissolved the Bi_2O_3, and was able to draw the CuO to the interface, allowing reaction to occur. Electrical testing showed the unfritted systems to exhibit increased dielectric losses at frequencies <10,000 Hz due to Pb loss resulting in interfacial polarisation.

Keywords: PZT; Electrodes; Ag

1. Introduction

Electrode metal pastes for electrical contact with electroceramics typically contain bonding additives to facilitate bonding at the metal–ceramic interface. For dielectric materials these additives usually fall into three main categories. *Frit* bonded pastes contain 2–10 wt.% of a glass frit, typically a borosilicate/aluminosilicate, its role being to melt, be drawn to the substrate by capillary action, wet the ceramic, and form a physical bond with the electrode metal. *Flux* bonded pastes contain 1–5 wt.% of a melting oxide phase (typically Bi_2O_3), its role being to be drawn to the metal–ceramic interface, and to wet and/or penetrate into the grain boundaries of the ceramic. *Reactive* bonded pastes contain a small amount (0.1–1 wt.%) of a reactive oxide, typically CuO or CdO, to facilitate reaction at the interface. *Mixed* bonded systems are probably the most commonly used, containing more than one (usually all) of these additives, the theory being, due to the empirical nature in which these technologies have evolved, that if one system works well, then there is further benefit in using the additives together. Much of the work done on the interaction of these additives with the substrates on which they are used has focused on the ceramics used for printed circuit board applications (e.g. Al_2O_3 and AlN). A series of studies of various binary glasses on perovskites such as $BaTiO_3$ and $CaTiO_3$[1–4] have been undertaken. In general, glasses rich in network formers (e.g. B_2O_3, SiO_2) facilitated reaction at the interface, whereas glasses rich in network modifiers (e.g. PbO, Bi_2O_3) did not.

The conduction mechanisms (and the effect on these of dopants) for lead zirconate titanate (PZT) have been studied by many authors.[5–7] It has been proposed[6] that the conductivity within undoped PZT is p-type, and that this resulted from vacancies on the Pb site, caused by the loss of PbO during sintering. These Pb vacancies become ionised (to promote localised electroneutrality), generating holes. Use of donor dopants also promotes Pb vacancies as well as contributing conduction electrons (reducing the p-type conductivity). The use of acceptor dopants (such as those used in the hard PZT

* Corresponding author. Tel.: +44 114 2225474; fax: +44 114 2225943.
E-mail address: w.e.lee@sheffield.ac.uk (W.E. Lee).

0955-2219/$ – see front matter © 2004 Elsevier Ltd. All rights reserved.
doi:10.1016/j.jeurceramsoc.2004.05.016

of this study) increase the number of oxygen vacancies, and contribute holes to the conduction process (increasing p-type conductivity). For this reason soft PZTs are more electrically insulating than hard PZTs.

Little published research has examined the microstructures of metal electrode–electroceramic interfaces and even less has correlated the microstructures to the electrical behaviour. Commercial hard PZTs were used along with 8 Ag-based electrode pastes of increasing complexity approaching commercial compositions. The Ag pastes contained from one to several oxide additions enabling the effect of each oxide and their synergistic effects on microstructures and electrical properties to be determined.

2. Experimental method

Commercial substrates of hard PZT doped with Sr and Fe, were polished and ultrasonically cleaned in methylated spirits. Ag based electrode metal pastes 1–8 with compositions given in Table 1 were screen printed on to the substrates. An organic vehicle containing two hydrocarbon resins, one cellulose resin, and two different grades of glycol solvents controlled the rheology of the electrode pastes. The samples were then fired using schedules comparable to those used in industry. From room temperature the samples were heated at 10 °C/min to 150 °C, held for 12 min to burn off the organic vehicle, heated at 10 °C/min to the target temperature (700, 800, and 900 °C), held for 1 h, before returning to room temperature at 10 °C/min. Samples were cut and polished in cross section, and sputter coated in carbon to avoid specimen charging. The microstructures of the electrode–electroceramic interfaces were then characterised using scanning electron microscopy (SEM) and energy dispersive spectroscopy (EDS). The SEMs used were a Camscan series 2A (operating at 20 kV), and a JEOL-6400 (operating at 20 kV), both with Link Analytical EDS systems (beryllium window) and capable of secondary and back-scattered electron imaging (SEI and BEI). A probe size of <0.05 μm diameter was used, with a likely interaction volume of <1 μm^3.

Samples were also produced for electrical testing. These samples consisted of 7.4 mm × 3.4 mm × 1.25 mm PZT blocks with fired screen printed electrodes of pastes 1–8 on each of the 7.4 mm × 3.4 mm faces. LCR measurements were performed on a Hewlett-Packard 4284A Precision LCR Meter. An ac field strength of ∼1V was used in each case. The dielectric loss (tan δ) was measured at frequencies of 20, 100, 1K, 10K, 100K, 500K, and 1 MHz, at room temperature. In between measurements made at each frequency, the machine was recalibrated with respect to open and short circuits to take into account frequency effects on impedance measurement. The electrical measurements were performed on two independently prepared samples for each system. The mean dielectric loss was then calculated from these two measurements.

Limited impedance spectroscopy measurements were undertaken to distinguish potential electrode effects. Room temperature performance was determined using a Hewlett-Packard HP 4192A LF Impedance Analyser. A single sample of each system was evaluated over the range 5 Hz to 2 MHz, with an ac amplitude of 100 mV, taking 10 measurements per decade, without bias. A single sample (paste 1/900 °C) was evaluated under the same conditions but with a dc bias of 5, 10, and 15 V. The data were analysed using in-house software, with the data corrected for sample geometry. This sample was also tested using a Solartron 1260 Impedance/Gain Phase Analyser, with a Solartron 1296 Dielectric Interface, to measure the impedance at an elevated temperature (102 °C), and at room temperature (for comparative purposes). An ac amplitude of 100 mV was used over the frequency ranges 1 Hz to 1 MHz, and 0.1 Hz to 100 Hz. The data corrected for sample geometry were analysed using Solartron Impedance measurement software.

3. Results and discussion

3.1. Microstructural analysis

For each electrode paste 1–8, fired at each temperature, EDS revealed some interchange of mass across the interface between the metal and ceramic, with Ag in the PZT and Pb, Zr, and Ti in the Ag electrode, local to the interface (∼1 μm). Diffusional penetration of Ag up to 1000 μm into PZT has been reported by Slinkina et al.[8] using a radio tracer method. EDS (detection limit >0.1 wt.% Ag) is unable to detect the low concentrations of Ag found by these authors at this depth (∼1000 μm) in the current work.

3.1.1. Unfritted pastes

Electrodes containing Ag alone (no bonding additives—paste 1) generally resulted in poor bonding, with extreme delamination (Fig. 1a) for samples fired at 700 °C, and significant interfacial cracking for samples

Table 1
Compositions of Ag-based electrode pastes 1–8

Paste	Composition	Paste	Composition
1	Ag	5	Ag + glass frit (∼8 wt.%)
2	Ag + Bi_2O_3 (5 wt.%)	6	Ag + Bi_2O_3 (5 wt.%) + glass frit (∼8 wt.%)
3	Ag + CuO (1 wt.%)	7	Ag + CuO (1 wt.%) + glass frit (∼8 wt.%)
4	Ag + Bi_2O_3 (5 wt.%) + CuO (1 wt.%)	8	Ag + Bi_2O_3 (5 wt.%) + CuO (1 wt.%) + glass frit (∼8 wt.%)

Glass frit composition ∼10 wt.% SiO_2, ∼13 wt.% Al_2O_3, ∼62 wt.% PbO, and ∼13 wt.% B_2O_3.

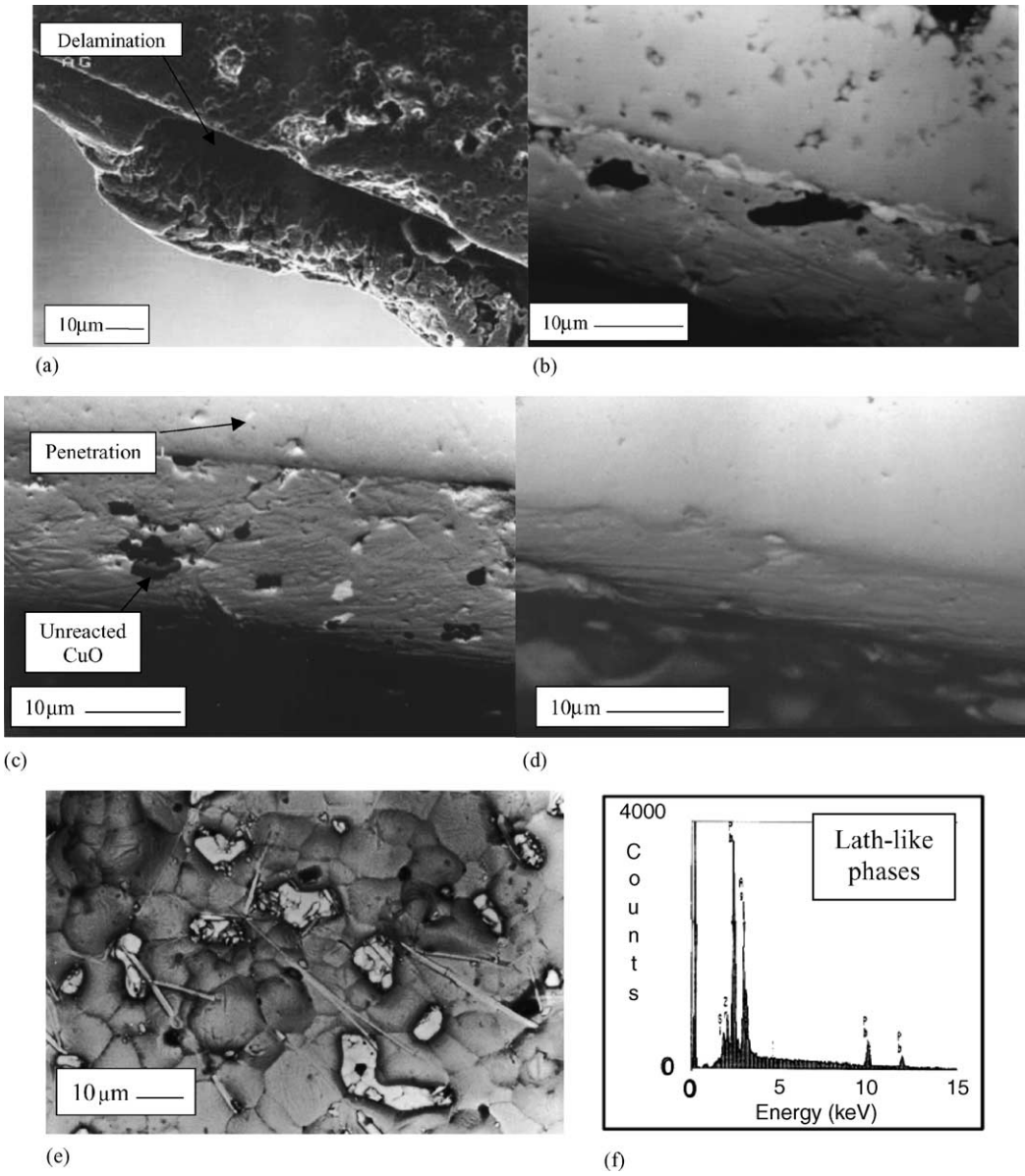

Fig. 1. (a) SEI of paste 1 (no additives) with extensive delamination (700 °C), (b) BEI of paste 2 (Ag + Bi_2O_3) showing an interfacial Bi-rich liquid (light phase) and limited grain boundary penetration (700 °C), (c) BEI of paste 4 (Ag + Bi_2O_3 + CuO) with deeper penetration of the Bi-rich phase, and prevalent unreacted CuO (700 °C), (d) BEI of paste 3 (Ag + CuO) with no CuO left in the bulk electrode (900 °C), and (e) BEI of the plan view microstructure of paste 3 (900 °C), showing the formation of light lath-like phases and (f) EDS of lath-like phases.

fired at 800 °C. By 900 °C the electrode adhesion improved, probably due to a Ag-PbO eutectic that is able to form from ~820 °C (Fig. 2). The effect of Bi_2O_3 is dependent on the presence of other additives and firing temperature. When Bi_2O_3 is the only bonding additive (paste 2), fired at 700 °C, a continuous Bi-rich (liquid) phase forms at the interface (Fig. 1b), penetrating the grain boundaries ~2 and 3 μm into the ceramic. Bi_2O_3 has a melting temperature of ~825 °C, which would suggest that the liquid phase is the result of a eutectic reaction, likely to be Bi_2O_3–PbO, which can form from ~600 °C. This continuous interfacial liquid phase is missing from the samples fired at 800/900 °C due to conditions more favourable to grain boundary penetration, with extensive penetration (>30 μm) of the Bi-rich phase into the PZT (similar to the microstructure shown in Fig. 1c). When Bi_2O_3 is included in the electrode paste with CuO (paste 4), the temperature of liquid formation appears lower. Samples fired at 700 °C (Fig. 1c) do not contain a continuous Bi-rich phase at the interface, with deeper grain boundary penetration of this Bi-rich liquid phase into the ceramic. A similar grain boundary penetrated microstructure is seen at 8/900 °C for paste 2.

The behaviour of CuO is less affected by the presence of Bi_2O_3. For pastes 3 and 4, unreacted CuO is abundant throughout the electrode microstructure (as seen in Fig. 1c) for samples fired at 700/800 °C. When fired at 900 °C there is

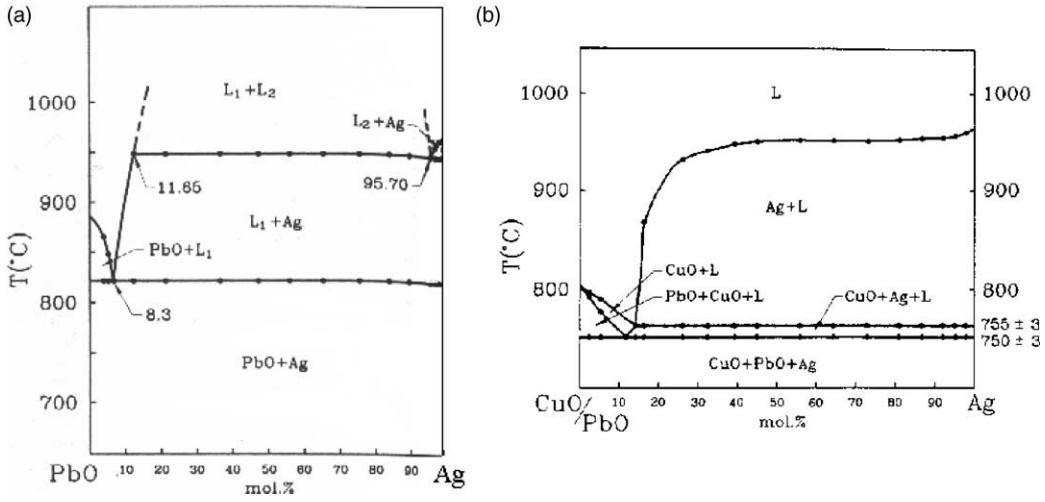

Fig. 2. (a) Phase diagram of the binary system PbO–Ag,[9] (b) pseudobinary Ag–PbO–CuO phase diagram with a 20CuO/80PbO molar ratio.[10]

a distinct difference, with no unreacted CuO within the electrode microstructure (Fig. 1d). Instead, EDS reveals traces of Cu in the electrode Ag itself, at the interface, and ~2–3 μm into the PZT. CuO, with a melting temperature of 1026 °C, would require interaction with other phases to melt. This change in state of CuO occurring between 800 and 900 °C may be due to a combination of the Ag–PbO eutectic (from ~820 °C)[9] and a Ag–PbO–CuO eutectic[10] (Fig. 2a and b), respectively, which can form from 750 °C. The formation of this lower temperature eutectic may not be possible at this temperature if the PbO levels in the bulk electrode are too low (if the process is kinetically slow). The formation of the Ag–PbO eutectic at the interface could be a pre-requisite, by facilitating increased transport of PbO into the electrode bulk, to making the melting of CuO possible. The detection of Cu within the PZT would suggest that interaction occurs with the ceramic in this melted state. Initial tests performed on the first reactive pastes in the 1970s (U.S. Patent 3 799 890) suggested that the optimum temperatures were the temperatures of decomposition of the reactive agent (1026 °C for CuO). The eutectic melting of CuO may lower the optimum temperatures by reducing the effective temperature of decomposition. Plan view analysis of the range of unfritted systems revealed the formation of lath-like grains on the surface of the electrode (Fig. 1e). These laths were found predominantly in sample fired at 900 °C, and some at 800 °C, and had a composition as shown in Fig. 1f. It is believed that these lath-like phases are PbO based (a result of PbO loss from the PZT substrate).

3.1.2. Fritted pastes

The firing temperature of the electrode affected the behaviour of the glass frit. In each case the presence (or otherwise) of B could not be detected, being too light an element for the Be window EDS detector, making Al, Pb and Si the detectable species. After firing at 700 °C the only element that could be detected by EDS was Al which was found throughout the electrode bulk. Since the glass frit was designed for firing at ~800 °C, the viscosity of the glass at 700 °C may be too high to flow through the network of pores to the electrode–ceramic interface. After firing at 800 °C the detectable glass frit elements (Pb, Al, Si) were all detected with increasing concentration as the interface was approached. This is generally accepted as the ideal scenario and would suggest that the glass is drawn towards, and interacts with, the substrate, perhaps by capillary action through the voids in the electrode microstructure. The interaction with the substrate and the glass is also known to have a role in drawing the frit to the interface. Yajima and Yamaguchi[11] found that a glass frit within a Ag electrode paste was preferentially drawn to an Al_2O_3 substrate, when compared to the frits behaviour on a Ag substrate, under identical conditions. The interaction of the frit with the Al_2O_3 was believed to be instrumental in this behaviour. After firing at 900 °C all of the detectable glassy elements were found, but dispersed throughout the electrode thickness. Plan view analysis (Fig. 3) of fritted systems fired at 900 °C showed phases likely to be glass on the surface of the PZT (seen through voids in electrode coverage), and on the electrode surface. Similar glass pools have been observed

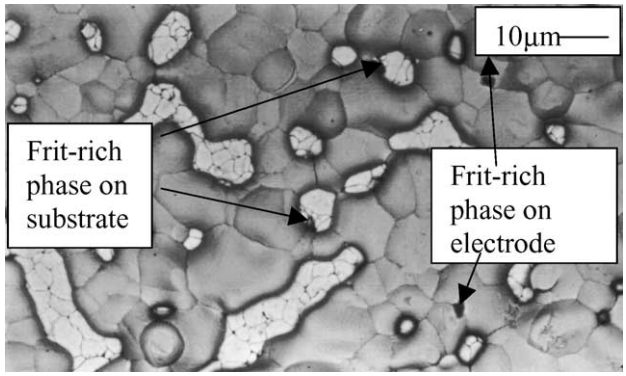

Fig. 3. Micrograph of the plan view microstructure of paste 3 fired on to the substrate at 900 °C, showing the lack of formation of lath-like phases.

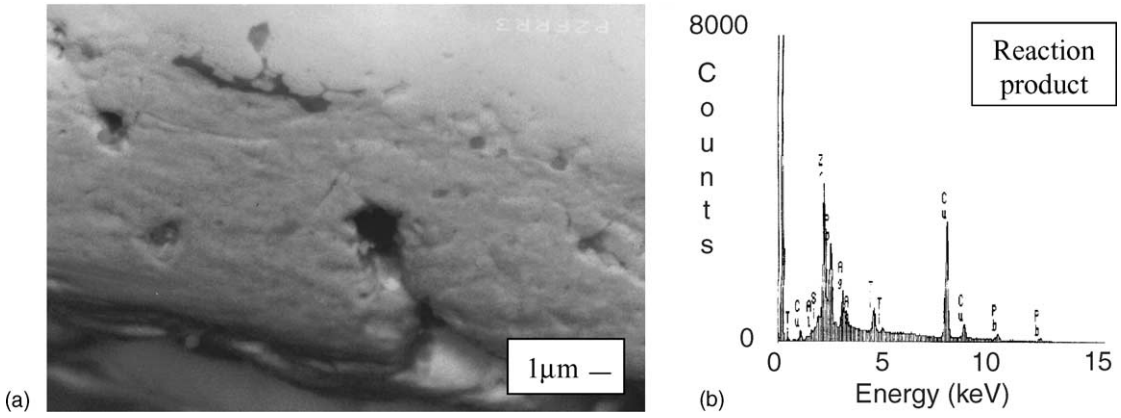

Fig. 4. (a) Electrode microstructure for paste 7 fired at 800 °C, showing a dark reaction product (EDS shown) (b) at the interface.

by Chung and Kim.[12] They found that by increasing the frit content within a Ag electrode the densification rate could be increased. The densification rate can also be increased by increasing temperature (reducing glass viscosity). The viscosity of a typical soda-lime-silica glass can change by a factor of 1000 over an interval of 100 °C,[13] which will have corresponding effects on the densification rate. This is why the temperature used for glass frit bonding should be controlled stringently. Plan view analysis also showed the fritted microstructures to be virtually free of the lath-like crystals seen for unfritted systems (Fig. 3).

The effectiveness of other additives when incorporated in fritted pastes was variable. The glass dissolved the Bi_2O_3 additions to the extent that Bi-rich phases were rare, even for samples fired at 700 °C. The efficiency of Bi_2O_3 as a bonding additive in this form is questionable, the bonding mechanism under these conditions is likely to be frit bonding, just by a modified glass composition. CuO is less easily dissolved, and is improved in effectiveness when used in tandem with the glass frit, which is able to draw the reactive oxide to the interface under certain conditions. Highly viscous glass may be too resistant to flow to reach the interface effectively, whereas low viscosity glass may be too fluid to draw the reactive oxide to the interface. When fired at 800 °C a dark non-continuous reaction product formed at the interface (Fig. 4a) and EDS (Fig. 4b) revealed it to be Zr- and Cu-rich. When fired at 700 °C, CuO is more prevalent in the electrode microstructure, which may be due to the glass being too viscous to perform this role effectively at this temperature, being designed for use just below 800 °C.

3.2. Electrical measurements

Graphs showing the dependence of dielectric loss on frequency for electrodes fired on to the substrates at 700, 800, and 900 °C, are shown in Fig. 5a–c, respectively, for pastes 1–8 (labelled P1–P8). In general, the fritted samples (P5–P8 in the graphs) experienced low losses (<0.004) with little dependence of frequency, or on the temperature of firing. This contrasted sharply with the unfritted samples, which exhibited significantly higher losses at lower frequencies (<10,000 Hz). The unfritted systems were also affected by differences in firing temperature, with a general increase in low frequency loss with temperature. Fig. 6a and b show representative room temperature plots of real and imaginary capacitance (C′ and C″) versus frequency for pastes 4 and 8, respectively (having been fired at each of the target temperatures). Fig. 6a (paste 4) is representative of unfritted sytems and Fig. 6b (paste 8) is representative of fritted systems. The plots show moderate variations in imaginary capacitance. The variations occur between samples fired at specific temperatures for particular pastes, primarily in unfritted systems, and occur at frequencies below 10^4–10^5 Hz. In fritted systems the variation in C″ is notably less. Fig. 7a shows room temperature plots of real and imaginary capacitance (C′ and C″) versus frequency for paste 1/900 °C, unbiased, and under dc biasing of 5, 10 and 15 V. The biasing in each case flattens the C″ curve. Fig. 7b shows unbiased plots of real and imaginary capacitance (C′ and C″) versus frequency for paste 1/900 °C, at room temperature and 102 °C, measured using a solartron dielectric interface. They show an order of magnitude increase in imaginary capacitance when measured at 102 °C.

4. Further discussion

Different composition electrolyte/insulator electrode interfaces polarise in various ways when subjected to an electric field.[14] A key feature, apart from the metal electrode composition, is the constitution of the grain boundaries within the PZT. The properties of the PZT grain boundaries local to the interface will be modified by migration of impurities introduced in the electrode.[8] In addition further rearrangement of dopants, vacancies, and other impurities/defects will arise on application of an electric field. The firing temperatures employed are above PZTs Curie temperature (<450 °C) so the component will be depoled. Even low concentrations of impurities can have a substantial effect on the properties although they may become concentrated at interfaces where the driving forces for diffusion are higher.[15]

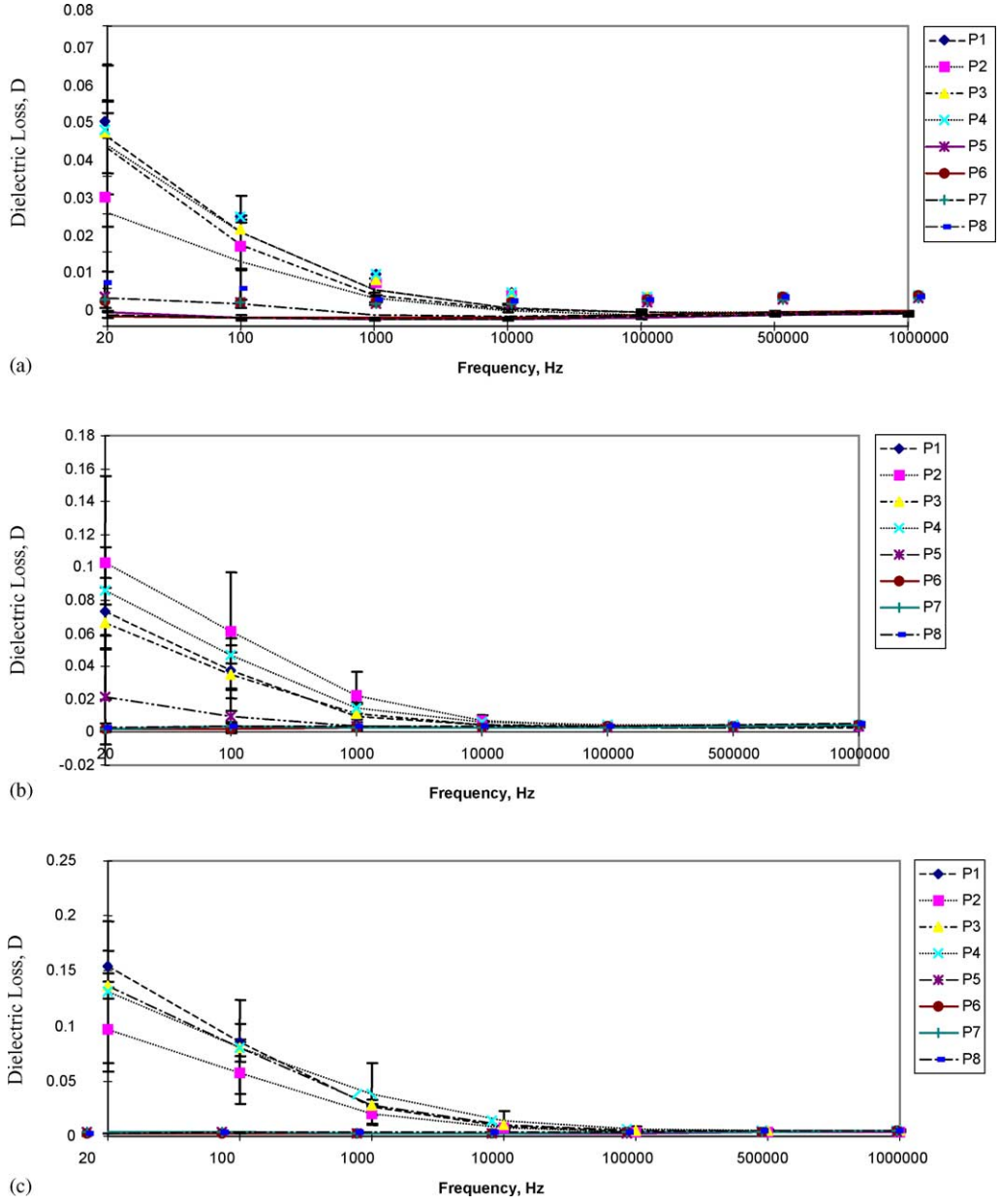

Fig. 5. Dielectric loss dependence on frequency for model pastes 1–8 for samples fired at (a) 700 °C, (b) 800 °C, (c) 900 °C.

A significant factor in PZT production is Pb loss. Zheng et al.[16] showed that Sr^{2+} dopants had a destabilising effect on the PZT, promoting PbO loss. Pb loss was a feature in each of the unfritted systems of this study. Indeed, formation of eutectics with PbO was a substantial feature in the microstructural development of these systems. Pb loss from PZT leaves cation vacancies within the perovskite crystal structure some of which are likely to be filled by Ag^{+} having similar ionic radii to Pb (Ag^{+} 1.26 Å, Pb^{2+} 1.20 Å). Slinkina et al.[8] examined diffusional penetration of Ag in PZT doped with Nb (soft PZT) concluding that most of the Ag penetration observed (after firing an Ag-coated pellet) was along PZT grain boundaries although they did not address Pb loss and potential diffusion of Ag^{+} into vacant Pb^{2+} sites. The reported increase in Ag content of the PZT from 500 to 750 °C could, however have been related to Pb loss.

Pb loss will produce structural Pb^{2+} vacancies and possibly O^{2-} vacancies depending on whether the Pb combines with oxygen ejected from the material or from the atmosphere. The mechanism by which dielectric loss occurs depends on the way in which charge neutrality is maintained when Pb^{2+} ions are lost from the PZT structure. Charge neutrality can be maintained in three ways. Firstly, by loss of O^{2-} (which combine with Pb^{2+} to form PbO). The presence of oxygen ions between cations and cation vacancies (and the energy barrier that would need to be overcome for the two to interchange) hinders conduction through cation migration. It follows that an increase in the number of oxygen

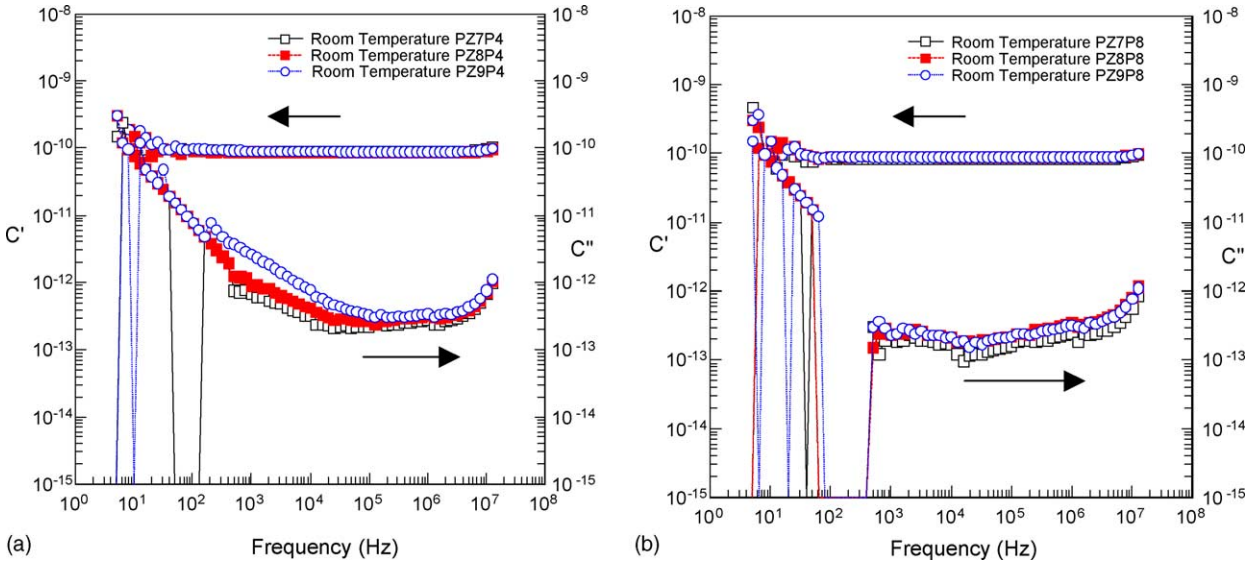

Fig. 6. Unbiased room temperature impedance spectroscopy measurements showing the response of C′ and C″ with frequency for (a) paste 4 (unfritted), and (b) paste 8 (fritted) samples. Units of C′ and C″ are F cm^{-1}.

vacancies, together with an increase in the number of cation vacancies would allow increased freedom of movement of Ag^{+}, O^{2-} and Pb^{2+} ions. Since in this study the samples had been heated above PZTs Curie temperature, had not been re-poled, and had been returned to room temperature at a slow rate, it can be assumed that a low energy configuration had been attained. However, as long as there is an increased number of Pb^{2+} vacancies and O^{2-} vacancies, then there is increased potential for ionic conduction. The number of O^{2-} ions lost from the structure may be lower than the number of Pb^{2+} ions (if Ag^{+} diffusion occurs or ionised vacancies occur). This means that there would be a requirement for recombination with further oxygen from the atmosphere to produce further PbO. This is energetically favourable, in air, at the temperatures investigated. Secondly, charge neutrality can be maintained by ionisation of vacancies left by the Pb^{2+}. Neglecting the effects of Ag^{+} diffusion, if more Pb^{2+} ions are lost from the PZT structure local to the electrode than O^{2-} ions then vacancies on the A site can become ionised (to promote electroneutrality), which generates holes. This phenomenon is believed to be a source of the p-type conductivity seen in PZT. Thirdly, charge neutrality can be maintained by

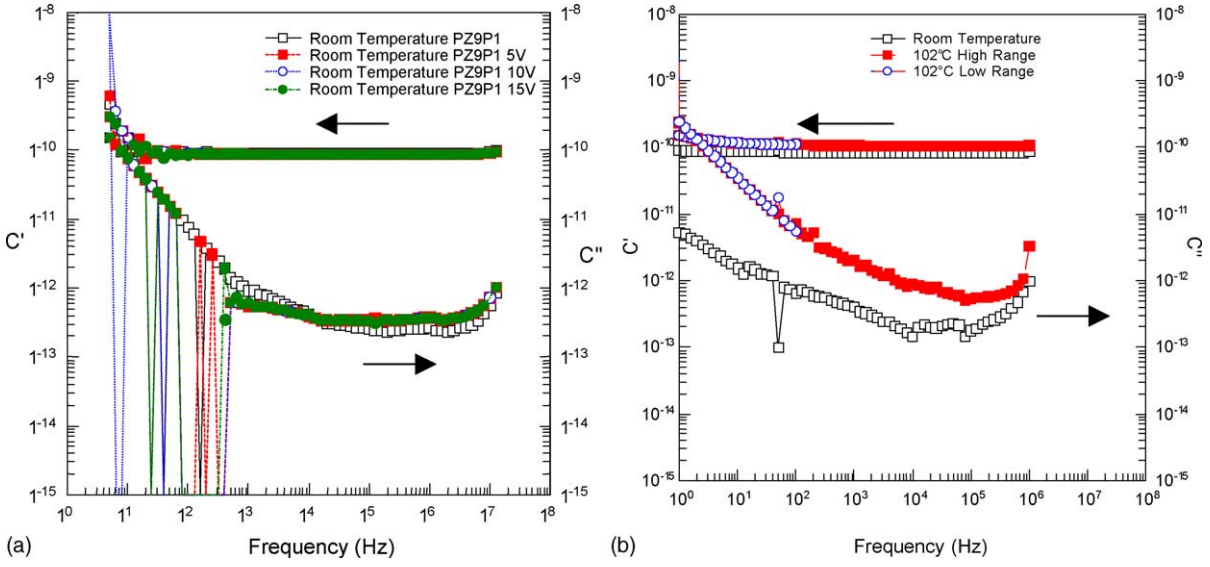

Fig. 7. Impedance spectroscopy measurements for sample with paste 1 fired at 900 °C showing the response of C′ and C″ with frequency for (a) room temperature measurements for unbiased, and for 5, 10 and 15 V dc bias, and (b) unbiased measurements at room temperature and 102 °C (using solartron dielectric interface). Units of C′ and C″ are F cm^{-1}.

a change in valency of remaining structural ions (e.g. Pb^{2+} to Pb^{4+}).[17] Both the Pb^{4+} ion and the vacancy can move under application of an electric field and so can contribute to ionic conduction. The location of Pb^{4+} ions on a Pb^{2+} site could also act as a donor impurity, which generates electrons, reducing p-type conductivity.

Since the Pb loss generally increased low frequency dielectric losses (increased conductivity) the first two of these processes are the most likely. There is potential for both ionic and hole conduction but the results of the present study do not allow these mechanisms to be distinguished. The dielectric loss behaviour does, however, suggest that a frequency dependent polarisation process (involving holes or ions) occurs predominantly in unfritted systems, resulting in increased losses at frequencies <10,000 Hz.

4.1. Trends in dielectric loss measurement

It is clear from the dielectric loss measurements taken of the 8 model paste systems fired at the three different temperatures (Fig. 5) that the addition of the glass frit substantially reduces the losses sustained in the lower frequency range, and also maintains these low losses as the firing temperature increases. To prove that these losses were real electrode effects further impedance analysis was undertaken. Much of the room temperature derived data, specifically in the C″ plot (versus frequency, Fig. 6), mirrored the general trends seen in dielectric loss. For unfritted systems there was a trend for C″ to increase with electrode firing temperature at frequencies below 10^4–10^5 Hz. For fritted systems the response of C″ is flatter across the lower frequency range, and is also less affected by firing temperature. These are both similar to the trends seen for dielectric loss measured with an LCR meter (Fig. 5).

dc biasing was used to further investigate the performance of paste 1/900 °C. Biasing in each case (Fig. 7a) flattened the C″ response effectively reducing C″ below 10^4–10^5 Hz. This could be the result of a reduction in losses. Measurements taken at 102 °C for paste 1/900 °C show that at higher frequencies bulk processes dominate but that at lower frequencies there are electrode effects (Fig. 7b) with significant increases in C″ when compared to measurements taken at room temperature. This indicates that the low frequency effects measured using the LCR meter to determine dielectric losses are actual electrode effects. The dielectric losses in unfritted systems were significantly higher at lower frequencies (<10,000 Hz) than those seen for fritted systems. In addition, as the firing temperature of the system was increased, there was a corresponding increase in lower frequency (<10,000 Hz) losses. In general, therefore, it appears that the loss mechanism is most effective at the lowest frequencies, becoming gradually less effective as the frequency of oscillation is increased, until a value of ∼10,000 Hz where it no longer has time to occur before the polarity is reversed again. Increasing the electrode firing temperature also appears to facilitate further losses.

4.2. Polarisation processes

In dipolar polarisation mechanism a vacancy (induced by an aliovalent dopant or impurity) effectively rotates around the impurity (which has an effective positive charge) as the metal ions hop onto it. This causes rotation of the dipole and is a source of dielectric loss at 10^3–10^6 Hz. The production of these dipoles could increase the losses due to dipolar rotation. However, these losses tend to peak at higher frequencies than those seen in this study. A second mechanism: interfacial polarisation, where charges (electrons or ions) pile up at intercrystalline boundaries, is relatively slow, usually taking place at frequencies <∼1Hz, but having some influence at up to 10^4 Hz. The explanation that fits best with the electrical data (Figs. 5–7) is that of interfacial polarisation consistent with greater levels of Pb^{2+} and oxygen vacancies which leads to enhanced Ag^+ and Pb^{2+} movement, or increased ionised vacancy (and hole) generation. This effect is similar to the dc conduction source of dielectric loss, the movement of charge carriers on application of an electric field, but with a barrier that will only allow carriers to travel a limited distance. As the field is reversed the charge carriers move in the opposite direction and the cycle begins again.

The dc biasing experiments undertaken (Fig. 7a) flattened the C″ response of the sample, effectively reducing C″ below 10^4–10^5 Hz indicating a reduction in dielectric loss. The use of dc biasing reduces the losses attributable to interfacial polarisation, since the mobile charge carriers would be drawn to, and held at, the boundary by the dc field. The low amplitude ac field would then have little impact in moving these mobile charge carriers away from the boundary against the dc field.

The microstructural and electrical evidence suggests that the presence of the glass frit in the electrode paste reduces Pb-loss. Potential reasons for this are: the vapour pressure of the glass frit (in particular the PbO within it) is higher than that of the PZT so hindering Pb loss from the PZT in a PbO-rich atmosphere; the presence of glass frit in the Ag electrode affects the concentration gradient of Pb/PbO at the interface and throughout the bulk electrode; and a simple physical sealing effect of the glass. The differences in Pb concentration profile will affect the diffusion kinetics at the interface. Ficks laws indicate that a concentration gradient is a driving force for diffusion. In the unfritted systems, since there is initially no Pb within the electrode, there will be a large concentration gradient at the interface which will be a driving force for Pb to diffuse into the electrode.

The combination of microstructural analysis and electrical measurements has detailed the individual effects of the inorganic additives used, and their performance in combination. The most significant additive is the glass frit which controls conditions at the interface governing electrical properties so that measured values were as expected for this grade of PZT. When other additives are used in combination with the glass frit they tend to dissolve in it, effectively producing

a frit with modified properties. This study suggests that for this application (Ag on PZT), reactive and fluxing additives (CuO and Bi_2O_3) are not required for good bonding and electrical performance. However, the CuO and Bi_2O_3 within the electrode composition are not expensive, and there is no evidence that they are detrimental to properties. Therefore there is little incentive to change the compositions of commercial systems. The unfritted electrodes used in this study produced lossy systems. In general, the higher the firing temperature, the more lossy the unfritted systems becomes. This, it is believed, is due primarily to PbO loss, which is only significant in PbO-containing ceramics. Furthermore, the increased losses within the unfritted systems always occurred at lower frequencies, which are not important for microwave dielectrics operated at higher frequencies.

5. Conclusions

- Inorganic additives are required for good adhesion, since delamination and cracking occurs in their absence for electrodes fired $\leq$800 °C.
- PbO loss is a significant phenomenon in the model electrode pastes studied and is the primary reason for property change. PbO is also the component from the substrate with which most of the electrode constituents interact to form liquid phases at lower temperatures. Eutectic reactions play an important role in unfritted systems.
- The electrical properties of the components were significantly improved by the glass frit. This is because the glass was able to reduce PbO loss. PbO loss introduced further vacancies within the PZT allowing increased movement of charge carriers (ions or holes). On application of an electric field this resulted in dielectric loss, believed to be due to interfacial polarisation, which is especially prevalent at lower frequencies.
- The behaviour of flux bonding additives varied considerably between fritted and unfritted systems. In unfritted systems Bi_2O_3 reacted with PbO to form liquid phases which flowed to the interface (at lower firing temperatures), and penetrated the substrate grain boundaries (at higher firing temperatures). In fritted systems Bi_2O_3 dissolved in the glass, resulting in a frit of modified composition.
- The behaviour of reactive bonding additives varied less between fritted and unfritted systems. In unfritted systems the CuO was in general ineffective in reaching the electrode–electroceramic interface at 7–800 °C. This was improved with the use of a glass frit which helped to facilitate transport of the CuO to the interface. At 900 °C CuO was dissolved by both fritted and unfritted electrode systems.

Acknowledgements

We thank Tim Adams and Dr. Derek Sinclair of the Department of Engineering Materials at the University of Sheffield for assistance with the Impedance Spectroscopy measurements and interpretation.

References

1. Yamaguchi, T., Ayaki, H. and Asai, L., Reaction of $CaTiO_3$ with PbO-B_2O_3 and PbO-SiO_2 Glasses. *J. Am. Ceram. Soc.*, 1993, **76**(4), 993–997.
2. Kuromitsu, Y., Wang, S. F., Yoshikawa, S. and Newnham, R. E., Interaction between barium titanate and binary glasses. *J. Am. Ceram. Soc.*, 1994, **77**(2), 493–498.
3. Kuromitsu, Y., Wang, S. F., Yoshikawa, S. and Newnham, R. E., Evolution of interfacial microstructure between barium titanate and binary glasses. *J. Am. Ceram. Soc.*, 1994, **77**(3), 852–856.
4. Hirata, A. and Yamaguchi, T., Interfacial reaction of $BaTiO_3$ with PbO-B_2O_3 glasses. *J. Am. Ceram. Soc.*, 1987, **80**(1), 79–84.
5. Wu, L., Wu, T.-S., Wei, C.-C. and Liu, H.-C., The DC resistivity of modified PZT ceramics. *J. Phys. C: Solid State Phys.*, 1983, **16**, 2823–2832.
6. Gerson, R. and Jaffe, H., Electrical conductivity in lead titanate zirconate ceramics. *J. Phys. Chem. Solids*, 1963, **24**, 979–984.
7. Dih, J. J. and Fulrath, R. M., Electrical conductivity in lead zirconate-titanate ceramics. *J. Am. Ceram. Soc.*, 1978, **61**, 448–451.
8. Slinkina, M. V., Dontzov, G. I. and Zhukovsky, V. M., Diffusional penetration of silver from electrodes into PZT ceramics. *J. Mater. Sci.*, 1993, **28**, 5189–5192.
9. Shao, Z. B., Liu, K. R. and Ling, Q. L., Equilibrium phase diagrams in the systems PbO-Ag and CuO-Ag. *J. Am. Ceram. Soc.*, 1993, **76**(10), 2663–2664.
10. Liu, H. K., Dou, S. X., Ionescu, M., Shao, Z. B., Liu, K. R. and Liu, L. Q., Equilibrium phase diagrams in the system CuO-PbO-Ag. *J. Mater. Res.*, 1995, **10**(1).
11. Yajima, K. and Yamaguchi, T., A further study on the microstructure of glass bonded Ag thick-film conductors. *IEEE Trans. Comp. Hybrids Manuf. Technol.*, 1984, **7**(3), 281–285.
12. Chung, Y. S. and Kim, H., Effect of oxide glass on the sintering behaviour and electrical properties in Ag thick films. *IEEE Trans. Comp. Hybrids Manuf. Technol.*, 1988, **11**(2), 195–199.
13. Scholze, H., *Glass—Nature, Structure and Properties*. Springer-Verlag, 1991.
14. MacDonald, J. R. and Johnson, W. B., Fundamentals of impedance spectroscopy. In *Impedance Spectroscopy: Emphasising Solid Materials and Systems*, ed. J. R. MacDonald. John Wiley and Sons , 1987.
15. Bernasik, A., Dupre, B., Janowski, J., Kowalski, K., Moya, E. G., Nowotny, J. *et al.*, Effect of segregation in ceramics. *Key Eng. Mater.*, 1995, **111/112**, 1–10.
16. Zheng, H., Reaney, I. M., Lee, W. E., Jones, N. and Thomas, H., Surface decomposition of strontium-doped soft $PbZrO_3$-$PbTiO_3$. *J. Am. Ceram. Soc.*, 2002, **85**(1), 207–212.
17. Eyraud, L., Eyraud, P. and Claudel, B., Influence of simultaneous heterovalent substitutions in both cationic sites on the ferroelectric properties of PZT type ceramics. *J. Solid State Chem.*, 1984, **53**, 266–272.